

ANALOGY BETWEEN MASS AND HEAT TRANSFER IN BEDS OF SPHERES: CONTRIBUTIONS DUE TO END EFFECTS

G. F. MALLING and GEORGE THODOS
Northwestern University, Evanston, Illinois

(Received 13 January 1966 and in final revised form 30 June 1966)

Abstract—Mass- and heat-transfer data obtained by the vaporization of water from porous spheres were used to calculate j -factors. Strict adiabatic conditions were employed for the attainment of solely fluid to particle transfer.

Fixed beds of several void fractions were constructed using short lengths of fine rigid wire to hold the spheres in regular geometrical orientations. In addition, the entrance and exit effects were eliminated by extending the ends of each bed with layers of inactive solid plastic spheres.

The resulting mass- and heat-transfer factors possessed a good correspondence indicating the existence of an analogy for these transfer processes. It was found that for the same Reynolds number the transfer factor, j , increased with the elimination of entrance and exit effects. The j -factors and the void fractions of the several beds, for which end effects were eliminated, produced with the Reynolds number the relationship. $\varepsilon^{1.19} j = 0.539/Re^{0.437}$ in the range $185 < Re < 8500$. This relationship is somewhat higher than that resulting from the data of Gamson, Thodos and Hougen and definitely lower than that proposed in 1963 by Sen Gupta and Thodos. Explanations for these differences are advanced.

NOMENCLATURE

A , constant, equation (5);
 c_p , heat capacity [Btu/lb degF];
 D_p , particle diameter [ft];
 D_v , diffusion coefficient [ft²/h];
 F , factor for axial dispersion, $\Delta p/(\Delta p)_m$;
 G , superficial mass velocity [lb/h ft²];
 G_i , average interstitial mass velocity (G/ε) [lb/h ft²];
 G_m , modified mass velocity (G/ε^2) [lb/h ft²];
 h_g , heat-transfer coefficient [Btu/h ft² degF];
 j , transfer factor, j_a or j_h ;
 j_a , mass-transfer factor, $\{[k_g p_{gf} M/G] [\mu/\rho D_v]_f^{\frac{1}{2}}\}$;
 j_h , heat-transfer factor, $\{[h_g/c_p G] [c_p \mu/k]_f^{\frac{1}{2}}\}$;
 j_i , εj ;
 j_m , $\varepsilon^2 j$;
 k , thermal conductivity [Btu/h ft degF];

k_g , mass-transfer coefficient [lb-mole/h ft² atm];
 M , molecular weight;
 n , exponent, $n = 1.19$, equation (2);
 p , partial pressure of water vapor [atm];
 p_{gf} , partial pressure of nontransferable component [atm];
 Pr , Prandtl number ($c_p \mu/k$);
 Re , Reynolds number ($D_p G/\mu$);
 Re_i , interstitial Reynolds number ($D_p G/\mu \varepsilon$);
 Re_m , modified Reynolds number ($D_p G/\mu \varepsilon^2$);
 Sc , Schmidt number ($\mu/\rho D_v$).

Greek symbols

α , exponent, equation (5);
 ε , void fraction;
 π , total pressure [atm];
 μ , viscosity [lb/h ft];
 ρ , density [lb/ft³].

Subscripts

i , inlet;

- m , log mean;
- o , outlet;
- w , surface.

CONSIDERABLE experimental information dealing with fluid particle mass and heat transfer for packed and distended beds of spheres has been presented in the literature over the last twenty years. For the most part, these efforts have dealt with the establishment of mass- and heat-transfer factors from experimental measurements involving liquid evaporation from the surface of porous spheres to a flowing gas. These studies have utilized beds of variable depth and in some cases attempts were made to minimize the entrance and exit effects.

Epstein [1] points out that different results can be expected for mass and heat transfer through shallow beds as compared with deep beds. Galloway *et al.* [2] studied the evaporation of water into air from porous spheres, 0.673 in. in diameter, and arranged in five different geometric orientations. To minimize end effects and simultaneously to avoid saturation of the air leaving the bed, they proposed as a compromise a bed having a depth of eight layers. Denton [3], Thoenes and Kramers [4], and Baldwin *et al.* [5] surround a single active sphere with a matrix of non-active spheres, thereby eliminating entrance and exit effects. Denton [3] compares the measurements obtained from a single sphere with the mass- and heat-transfer data resulting from packed beds of active spheres and concludes that the two systems produce essentially the same results. While these investigators recognize the contributions of end effects and attempt to eliminate them, they make no direct effort to show quantitatively the contributions of these effects to the transport of mass and heat in fixed beds.

In addition, the recent work of Sen Gupta and Thodos [6] shows that an analogy between mass and heat transfer exists in the flow of gases through packed and distended beds of spheres, and their work produced j -factors that were somewhat higher than those found in earlier

studies [7]. To minimize radiant heat transfer, Sen Gupta and Thodos adjusted the temperature of the surroundings to that of the wet spheres in the bed. Although this approach proved helpful in minimizing this contribution, it did not take into account the convective heat transfer from the flowing air to the walls of the cartridge containing the bed. Furthermore, in their work, the air entered the chamber through oblique openings immediately above the bed, which was responsible for the generation of an increased level of turbulence. Galloway and Sage [8] point out that the level of turbulence has a marked effect on the rates of mass and heat transfer from a single sphere to a fluid flowing past it. A similar behavior is to be expected for a fluid flowing through a packed bed. Furthermore, in the work of Sen Gupta and Thodos [6] the air unavoidably must have approached the bed as a series of oblique jets, thus generating a flow pattern that was unique to their study.

The issues concerning the convective heat flow from the air to the walls of the cartridge, and the uncertainty involving the flow pattern and degree of turbulence of the air entering the bed warrant an experimental re-examination which should take into account not only end effects, but at the same time should consider the points of doubt existing in the mass- and heat-transfer analogy as proposed by Sen Gupta and Thodos [6].

EXPERIMENTAL PROCEDURE AND EQUIPMENT

1. The experimental apparatus consisted of a chamber constructed of brass, 16 in high and having a squared cross section, 7 × 7 in. This unit was completely water-jacketed and is diagrammatically presented in Fig. 1. The interior of this chamber was accessible through a hinged door at the front. This door was also water-jacketed and when closed against a sponge Neoprene gasket, the interior was completely isolated from the ambient environment. To insure a uniform temperature distribution, the walls of the chamber and the door were provided

with internal baffles which directed the water to flow upward through a series of horizontal reverses. A prescribed temperature at the walls of the chamber was maintained by recirculating water from a constant temperature bath.

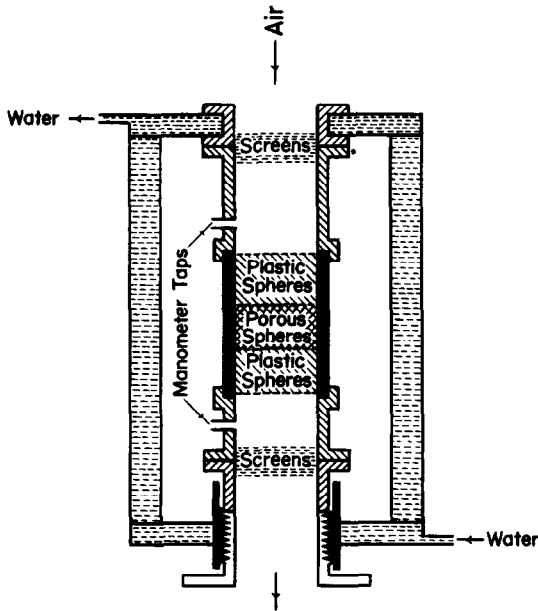


FIG. 1. Schematic diagram of water-jacketed chamber and test section.

2. Air-flow rates were determined with a system of three rotameters, connected in parallel. Conditioned air at atmospheric pressure was directed downward through the test section. The humidity of the inlet air was established by diverting a small fraction of the inlet air to the rotameters and expanding it to atmospheric pressure before introducing it to a unit equipped with wet and dry bulb thermometers.

The test section consisted of a section of plastic pipe, i.d. = 3.72 in. This was positioned between two similar plastic pipes of the same diameter. The upper pipe was coupled to a brass tube which was permanently attached to the top of the chamber. The lower section also consisted of a plastic pipe which was bolted to a telescoping brass fitting attached to the base of the chamber. The bottom pipe could be raised or lowered a

short distance by turning an external flange which permitted the test section to be fixed in place or to be removed as required. Ten layers of screen, at the inlet of the unit, were used to produce a uniform gas flow. The pressure difference was measured with a micromanometer having a resolution of 0.0001 in. of manometer fluid (isobutyl alcohol). To minimize radiant heat transfer to the active spheres, their immediate surroundings were sprayed with bright aluminum paint.

3. The beds were made of porous spheres, 0.617–0.625 in. in diameter. These spheres were capable of absorbing sufficient quantities of water to exhibit constant drying rates. Several spheres were provided with fine copper–constantan (No. 36 gage) wire thermocouples by drilling through a major diameter and inserting the wires through the hole until the junction reached a point just below the opposite surface.

4. Water was evaporated from the surface of these spheres into the air passing through the voids of the packed and distended beds. Two distended beds were used. Each of these beds consisted of six layers of spheres, 0.625 in. in diameter, which were held in a body-centered cubic lattice. The spheres were separated with short lengths of fine rigid wire capable of supporting this structure. Each distended bed was provided with a removable entrance section of three layers and an exit section of two layers of solid plastic spheres. These spheres were also separated with fine rigid wires and were also oriented in a body-centered cubic lattice.

Each test section included the active spheres and the entrance and exit sections. The void fraction of each bed studied is presented in Table 1. The void fraction of the bed of active spheres without end layers was obtained using the total volume included between the overall height of the entire bed. For distended beds with both end sections, the void fraction was taken between the midpoint of the top and bottom layers of spheres in the active portion of the bed.

To minimize wall effects, the peripheral spheres were properly segmented to fit the

Table 1. Void fractions and geometric arrangement of packed and distended beds of spheres

Layers of spheres				ϵ
Entrance section	Active bed	Exit section		
A. Packed Beds				
(a)		1		0.517
(b)		1	1	0.435
(c)	1	1		0.435
(d)	3	1	2	0.366
(e)	3	3	2	0.386
B. Distended Beds				
(a)		6		0.582
(b)	3	6	2	0.545
(c)		6		0.794
(d)	3	6	2	0.788

inside cylindrical surface of the test section. To exclude the cylindrical surfaces of the segmented spheres from mass and heat transfer, a thin coat of nonporous epoxy resin was applied to them. The spheres of the entrance and exit sections in the periphery were segmented in a similar manner.

5. The packed beds were formed by stacking layers of active spheres and layers of solid plastic spheres. Each of these layers was held together with short lengths of fine rigid wire which joined the points of contact of the spheres. Active and inactive spheres were machined peripherally to conform to the cylindrical surface of the test section. With this arrangement, the five different packed beds presented in Table 1 were constructed. The fixed bed with the three active layers of spheres and the two distended bed orientations, including their entrance and exit sections, are presented in Fig. 2.

System temperatures were measured with copper-constantan thermocouples using an Elektronik potentiometer accurate to about 0.1 degF. The thermocouples, imbedded in the spheres of the test section, were connected to a multipoint plug, mounted on the inside of the chamber, which could be disengaged so that each bed could be removed for periodic weighings.

A typical run consisted of subjecting a bed of spheres saturated with water to drying by forcing conditioned air through the interstices of each packing. In the course of a run, the temperature of the air entering the test section was controlled to within 0.1 degF of a prescribed value. To realize essentially adiabatic conditions, the temperature of the water passing through the chamber walls was adjusted to the average dry-bulb temperature of the air flowing through the bed. At regular time intervals (5-30 min), the air flow was stopped and the bed was weighed. This procedure was repeated in order to establish the constant rate of drying. The results and basic information of each run are presented elsewhere [9].

RESULTS

Altogether 100 experimental runs were carried out using the packed and distended bed arrangements. The information gathered from these runs permitted the calculation of the transfer coefficients, k_g and h_g , and their corresponding dimensionless transfer factors, j_d and j_h . The calculational procedure for these quantities is identical to that described elsewhere [7]. For the establishment of k_g , the partial pressure difference across the film

$$(\Delta p)_m = \frac{\frac{p_o}{\pi - p_o} - \frac{p_i}{\pi - p_i}}{\frac{\pi}{\pi - p_w} \left[\frac{1}{\pi - p_i} - \frac{1}{\pi - p_o} + \frac{1}{\pi - p_w} \ln \frac{(\pi - p_o)(p_w - p_i)}{(\pi - p_i)(p_w - p_o)} \right]} \quad (1)$$

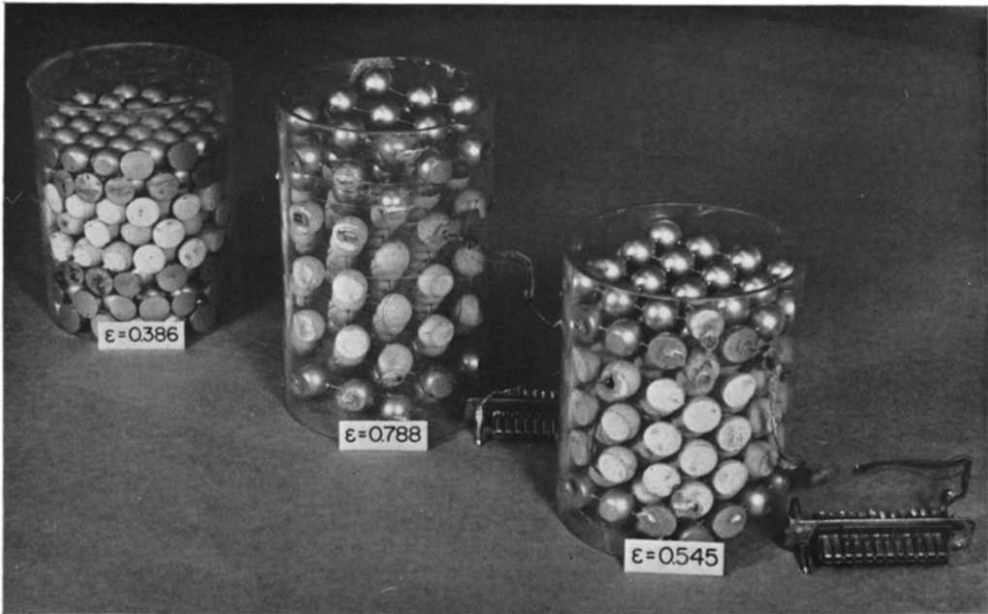


FIG. 2. Close-up view of test sections consisting of packed and distended beds of active spheres and layers of solid plastic spheres at the inlet and outlet of each bed.

was used. The correct driving force, $\Delta p = F(\Delta p)_m$, takes into account the presence of axial dispersion as outlined by Epstein [1]. However, in the analysis of the data of this study, the introduction of the F -factor does not change the relative position of the relationships involving entrance and exit effects or number of active layers of spheres present in each fixed bed. Therefore, this correction was not introduced until the results of this study were compared with existing packed bed data available in the literature.

For these runs, the Prandtl group at average film conditions was found to vary from $Pr = 0.712$ to $Pr = 0.714$ while the Schmidt group varied from $Sc = 0.607$ to $Sc = 0.611$. Other pertinent physical properties can be found elsewhere [9]. The air flow rates produced Reynolds numbers that ranged from $Re \approx 100$ to $Re \approx 8500$. In these calculations the heat-transfer factors exhibited better internal consistency and therefore were considered to be more reliable. This choice stems from the fact that the vapor pressure of water varies exponentially with the measured surface temperature. Consequently, a small discrepancy in the surface temperature

results in a significant error on the vapor pressure calculated for water at surface conditions. Therefore, the resulting j_h values are inherently more reliable.

Packed beds (single active layer)

For the experimental runs associated with a single layer of active spheres, the resulting j vs. Re relationships are presented in Fig. 3. In general, the j_d and j_h values of each run were sufficiently close to indicate the existence of an analogy between mass and heat transfer. Therefore, these factors have been directly related to Re to obtain single relationships for both types of transport. The single layer of active spheres alone produced essentially equivalent j_d and j_h values which were used to obtain the lowest relationship of Fig. 3. With the introduction of a single layer of solid plastic spheres immediately after the active layer, this relationship shifted upward. For this arrangement, the greatest departure between j_d and j_h values was encountered and, for the most part, the j_h values were used to establish the dependence of j on Re . When the layer of solid plastic spheres was placed before the layer of active spheres, a more

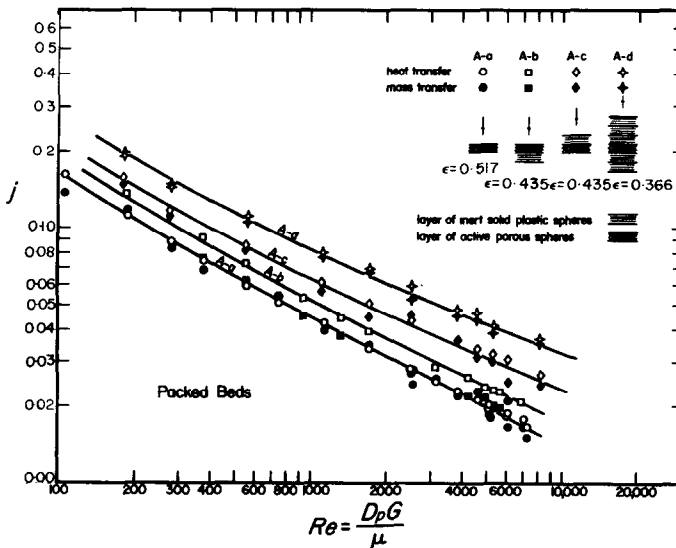


FIG. 3. Relationships between j and Re for a single layer of spheres with variable end conditions.

pronounced increase in the j -factor shift was observed. This arrangement exhibited a good j_d and j_h analogy. When the active layer of spheres was included between five layers of solid plastic spheres, three preceding and two following the active layer, the most pronounced increase in j_d and j_h values was encountered. The resulting j_d and j_h values show a good mass- and heat-transfer correspondence and both were used to develop the j vs. Re relationship for this arrangement. The increased rates of transfer found to exist with the presence of the solid plastic spheres can be attributed to the greater level of turbulence generated as the air entered the active layer of spheres. In addition, with the introduction of overlapping layers of spheres, the void fraction of the bed decreased, giving rise to an increased interstitial air velocity.

Distended beds (active spheres only)

Each of the two distended beds was comprised of six layers of active spheres, 0.625 in. in diameter. These spheres were oriented in a body-centered cubic lattice and were held in place with fine rigid wires. These beds have void fractions of $\epsilon = 0.582$ and $\epsilon = 0.794$ and consisted entirely of spheres participating in mass and heat transfer. The j_d and j_h values obtained from these two distended beds are related to Re to produce the relationships presented in Fig. 4. The distended bed having $\epsilon = 0.582$ produced j_d and j_h values that exhibit a close correspondence to mass and heat transfer and which permit a smooth curve to be drawn through them. On the other hand, the more distended bed, $\epsilon = 0.794$, gave rise to j_h values that were consistently higher than the corresponding j_d values. This disparity appears to be associated with beds of high void fractions which give rise to irregular temperature profiles as the air leaves the bed. Both of these distended beds are relatively short and consequently include end effects.

Distended beds (no end effects)

The end effects of the two distended beds of active spheres were eliminated by extending each

bed with three layers of solid plastic spheres at the inlet and with two such inactive layers at the outlet. Because of the overlapping of the adjacent layers of active and plastic spheres, the void fractions of these two beds decreased from $\epsilon = 0.582$ to $\epsilon = 0.545$ and from $\epsilon = 0.794$ to $\epsilon = 0.788$. The resulting j_d and j_h factors for the distended bed with $\epsilon = 0.545$ exhibited excellent correspondence, as indicated in Fig. 5. The more distended bed with $\epsilon = 0.788$ produced j_d and j_h values that did not exhibit as good a correspondence in the low Reynolds number region. The lack of good correspondence for this distended bed is consistent with the findings

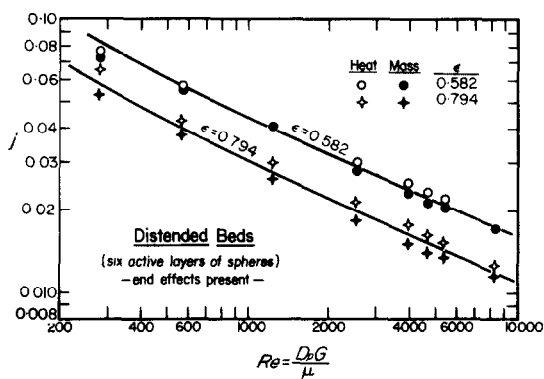


FIG. 4. Relationships between j and Re for two distended beds consisting of only active spheres.

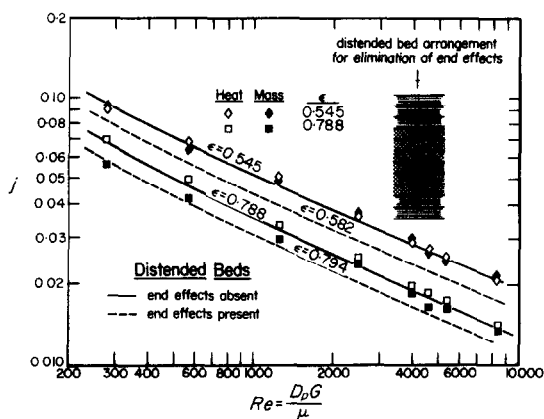


FIG. 5. Relationships between j and Re for two distended beds of active spheres included between layers of inactive solid plastic spheres.

exhibited when end effects were present for this bed. For comparative purposes, the relationships of Fig. 4 have been included in Fig. 5 as dotted curves. The elimination of the end effects increases on the average the j -factors approximately 20 per cent for the less distended bed and approximately 15 per cent for the more distended bed of spheres.

*Effect of bed depth on transport
(packed beds—no end effects present)*

The results obtained for the single active layer of spheres preceded by three layers and followed by two layers of solid plastic spheres, presented in Fig. 3, are compared in Fig. 6 with the results obtained for a similar system but consisting of three layers of active spheres. The resulting j_d and j_h values for this three-layer bed, with end effects eliminated, indicate the existence of a mass- and heat-transfer analogy. The relationships for these two beds are nearly equivalent and probably would have been identical if the void fractions of these two beds were equal. This close agreement indicates that the j -factors are essentially independent of bed height, provided that end effects are eliminated. This is a rather interesting and surprising conclusion drawn from this experimental evidence.

**CONTRIBUTION OF VOID FRACTION TO
MASS AND HEAT TRANSFER**

To investigate the effect of ϵ on both mass and heat transfer, this variable has been related to both j and Re to obtain a relationship that includes all three variables. For this analysis, j -factors for both packed and both distended beds, having no end contribution, were considered. One of the three methods of correlating these data involved the dependence of the product $\epsilon^2 j$ on $Re = D_p G / \mu$. A least-squares analysis in which the percentage deviations in ϵ , j , and Re were minimized, produced the following relationship

$$\epsilon^{1.19} j = \frac{0.539}{Re^{0.437}} \quad (2)$$

Equation (2) reproduces the experimental values of j with a root-mean-square deviation of 5.3 per cent.

Another way of correlating this information involved the use of the interstitial mass velocity,

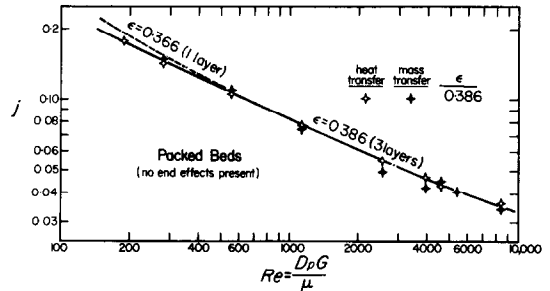


FIG. 6. Comparison of j vs. Re relationships for packed beds consisting of one and three active layers of spheres (no end effects present).

$G_i = G/\epsilon$ in place of G , the superficial mass velocity as utilized by Carberry [10] and McCune and Wilhelm [11]. Using G_i , the Reynolds number becomes $Re_i = D_p G / \mu \epsilon$ and the transfer factor becomes $j_i = \epsilon j$. A method of least-squares analysis which minimizes the percent deviations in ϵ , j , and Re_i , yielded the relationship,

$$\epsilon^{0.63} j_i = \frac{0.539}{Re_i^{0.437}} \quad (3)$$

Values of $\epsilon^{0.63} j_i$ and Re_i obtained from the experimental runs of the packed and distended beds are related in Fig. 7. A proper rearrangement of the variables of equation (3) produces the identical form of equation (2).

The use of a modified mass velocity defined as $G_m = G/\epsilon^2$ results in a modified transfer factor $j_m = \epsilon^2 j$ and a modified Reynolds number, $Re_m = D_p G / \mu \epsilon^2$. When equation (2) is rearranged to conform to these definitions, the following expression results:

$$\epsilon^{0.064} j_m = \frac{0.539}{Re_m^{0.437}} \quad (4)$$

Equation (4) shows that j_m is essentially independent of ϵ and therefore this equation can be

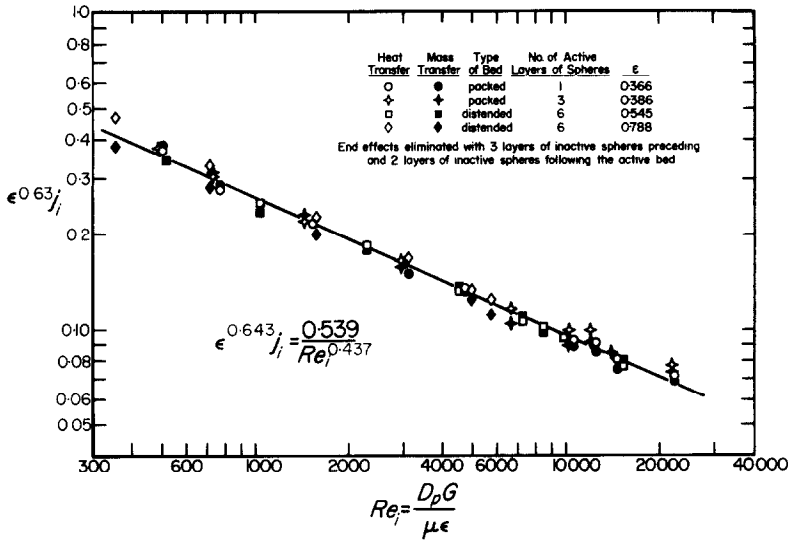


FIG. 7. Dependence of $\epsilon^{0.63}j_i$ of Re_i for packed and distended beds of spheres (no end effects present).

assumed to be of the form

$$j_m = \frac{A}{Re^x} \tag{5}$$

A least-squares analysis of the data establishes the constants of equation (5) to be

$$j_m = \frac{0.534}{Re^{0.431}} \tag{6}$$

The Reynolds number $Re = D_p G / \mu$ utilizes a superficial mass velocity that is independent of the interstitial nature of the bed and properly defines the transfer process for different beds as long as their void fractions remain the same. A variation in the void fraction does not necessarily produce an effective mass velocity, $G_i = G/\epsilon$, which is applicable to both the laminar and turbulent regimes. However, $G_i = G/\epsilon$ has been shown by Carberry [10] to apply to packed beds for $0.50 < Re_i < 900$. At high flow rates the void fraction dependence is approximated by $G_m = G/\epsilon^2$, as indicated by equation (6). Equations (2), (3), and (4) are equivalent and produce a mean deviation of 5.3 per cent in j . This deviation increases to

5.9 per cent when the data are correlated in terms of j_m and Re_m in accordance with equation (6).

COMPARISON OF RESULTS

The results of this study for the two packed and two distended beds expressed through equation (2) are presented in Fig. 8. When these results are corrected for axial dispersion, this linear relationship becomes

$$\epsilon^{1.19}j = \frac{0.763}{Re^{0.472}} \tag{7}$$

obtained from the experimental data of other investigators. In these comparisons, $\epsilon^{1.19}j$ is related to Re as shown in Fig. 8. The j -factor relationships of Gamson *et al.* [7] for mass and heat transfer have been combined to produce the dependence of $\epsilon^{1.19}j$ on Re for the experimental work reported by them in 1943. Their results fall about 20 per cent below the correlation of the present study. This behavior is not unexpected in view of the fact that their relationship includes end effect contributions

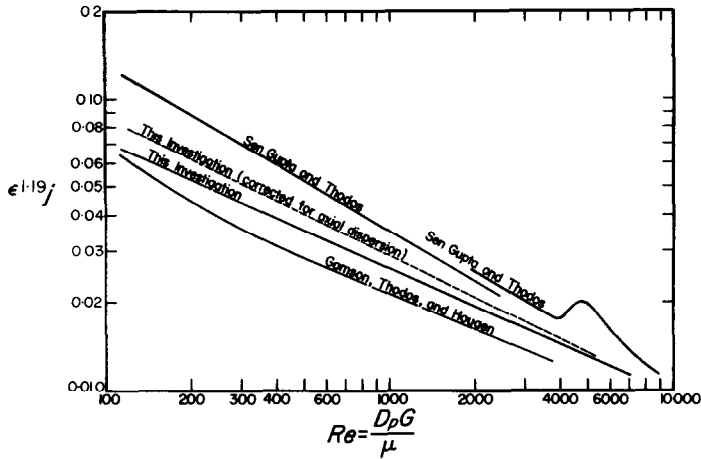


Fig. 8. Comparison of $\epsilon^{1.19}j$ vs. Re relationships resulting from this investigation and those of others for fixed beds of spheres.

which have been eliminated in the data used to obtain equation (2). On the other hand, the mass- and heat-transfer data of Sen Gupta and Thodos [6] produce a relationship that is considerably higher despite the fact that the same distended beds used in this study had been used by them. However, the beds used by Sen Gupta and Thodos [6] did not include any entrance and exit sections. A careful review of their experimental technique indicates that the air approached their beds as a series of oblique jets which undoubtedly gave rise to a considerably higher degree of turbulence that would be produced if entrance and exit sections were present, and hence the higher mass- and heat-transfer factors.

The experimental runs of this investigation covered a range of Reynolds numbers from $Re \approx 180$ to $Re \approx 8500$. In this interval, the $\log(\epsilon^{1.19}j)$ vs. $\log Re$ relationship was essentially linear without the encounter of a transition point at $Re \approx 4800$ as reported by Sen Gupta and Thodos [12].

ACKNOWLEDGEMENT

The authors acknowledge the support of the Esso Education Foundation for the fellowship which made this study possible.

REFERENCES

1. N. EPSTEIN, *Can. J. Chem. Engng* **36**, 210 (1958).
2. L. R. GALLOWAY, W. KORMARNICKY and N. EPSTEIN, *Can. J. Chem. Engng* **35**, 139 (1957).
3. W. H. DENTON, *Proceedings of the General Discussion on Heat Transfer*, pp. 370-373. Inst. Mech. Engrs. (London) and Am. Soc. Mech. Engrs. (September 1951).
4. D. THOENES and H. KRAMERS, *Chem. Engng Sci.* **8**, 271 (1958).
5. D. E. BALDWIN, R. B. BECKMANN, R. R. ROTHFUS and R. I. KERMODE, *Ind. Engng Chem. (Process Design and Development)* **5**, No. 3, 281 (1966).
6. A. SEN GUPTA and G. THODOS, *A.I.Ch.E. Jl* **9**, 751 (1963).
7. B. W. GAMSON, G. THODOS and O. A. HOUGEN, *Trans. Am. Inst. Chem. Engrs* **39**, 1 (1943).
8. T. R. GALLOWAY and B. H. SAGE, *Int. J. Heat Mass Transfer* **7**, 283 (1964).
9. G. F. MALLING, Ph.D. dissertation, Northwestern University, Evanston, Ill. (1965).
10. J. J. CARBERRY, *A.I.Ch.E. Jl* **6**, 460 (1960).
11. L. K. MCCUNE and R. H. WILHELM, *Ind. Engng Chem.* **41**, 1124 (1949).
12. A. SEN GUPTA and G. THODOS, *Ind. Engng Chem. (Fundamentals)* **3**, 218 (1964).

Résumé—Les données de transport de masse et de chaleur obtenues par vaporisation de l'eau à partir de sphères poreuses ont été utilisées pour calculer les facteurs j . On a employé des conditions rigoureuses d'adiabaticité afin d'obtenir seulement le transport du fluide à la particule.

On a fabriqué des lits fixes avec plusieurs fractions de vides en employant des fils fins, rigides et courts pour maintenir les sphères dans des orientations géométriques régulières. De plus, les effets d'entrée

et de sortie ont été éliminés en prolongeant les extrémités de chaque lit avec des couches de sphères solides en matière plastique inactive.

Les facteurs résultants de transport de masse et de chaleur correspondaient bien entre eux, ce qui indique l'existence d'une analogie pour ces processus de transport. On a trouvé que pour le même nombre de Reynolds le facteur de transport, j , augmentait lorsqu'on éliminait les effets d'entrée et de sortie. Les facteurs j et les fractions de vide de plusieurs lits, pour lesquels on avait éliminé les effets d'extrémités, étaient reliés au nombre de Reynolds par la relation: $\varepsilon^{1.19} j = 0,539/Re^{0.437}$, dans la gamme $185 < Re < 8500$.

Cette relation est quelque peu plus élevée que celle provenant des données de Gamson, Thodos et Hougen et effectivement plus basse que celle proposée en 1963 par Sen Gupta et Thodos. Des explications pour ces différences sont fournies.

Zusammenfassung—Zur Berechnung von j -Faktoren wurden Daten des Wärme- und Stoffüberganges zugrundegelegt, die bei der Verdampfung von Wasser an porösen Kugeln erhalten wurden.

Festbetten unterschiedlicher Schüttverhältnisse wurden konstruiert, wobei kurze steife Drähte die Kugeln in regelmässigen Anordnungen hielten. Ausserdem wurden die Eintritts- und Austrittswirkungen ausgeschaltet, indem die Enden jedes Bettes aus Lagen inaktiver, fester Plastik-Kugeln gebildet wurden.

Die resultierenden Wärme- und Stoffübergangsfaktoren wiesen eine gute Übereinstimmung auf, was die Existenz einer Analogie zwischen den Vorgängen andeutet. Es ergab sich, dass bei gleichbleibender Reynolds-zahl der Übergangsfaktor j zunahm, wenn Eintritts- und Austrittseinflüsse ausgeschaltet wurden. Die j -Faktoren und die Schüttverhältnisse für die verschiedenen Betten, deren Randeinflüsse ausgeschaltet waren, wiesen im Bereich $185 < Re < 8500$ folgende Abhängigkeit von der Reynolds-zahl auf $\varepsilon^{1.19} j = 0,539/Re^{0.437}$. Diese Beziehung liefert Werte, die etwas höher liegen als jene von Gamson, Thodos und Hougen und tiefer als die im Jahre 1963 von Sen Gupta und Thodos vorgeschlagenen. Erklärungen für diese Unterschiede sind gegeben.

Аннотация—Данные по переносу массы и тепла, полученные при испарении воды из пористых шариков, использовались для расчёта значений коэффициента j . Для того чтобы перенос происходил только от газа к частицам, поддерживались строго адиабатические условия.

Были изготовлены неподвижные слои с различной порозностью. Для того чтобы шарики располагались геометрически правильно, их укрепляли на короткой тонкой упругой проволоке. Кроме того, эффекты на входе и выходе устранялись путем удлинения концов каждого слоя слоями неактивных твердых пластических шариков.

Полученные коэффициенты переноса массы и тепла оказались в хорошем соответствии, что указывает на существование аналогии между этими процессами переноса. Найдено, что при тех же значениях критерия Рейнольдса коэффициент переноса j возрастал при устранении эффектов на входе и выходе. При исключении концевых эффектов опытные данные обобщаются соотношением $\varepsilon^{1.19} j = 0,539 Re^{0.437}$ проверенным в диапазоне $185 < Re < 8500$. Это соотношение несколько превышает соотношение, полученное по данным Геймеона, Тодоса и Гугена, и является значительно ниже соотношения, предложенного в 1963 году Сен Гунтой и Тодосом. Предложено объяснение этого расхождения.